

# Light $\Xi$ hypernuclei in four-body cluster models

E. Hiyama

*Nishina Center for Accelerator-Based Science, Institute for Physical and Chemical Research (RIKEN), Wako, Saitama, 351-0198, Japan*

Y. Yamamoto

*Physics Section, Tsuru University, Tsuru, Yamanashi 402-8555, Japan*

T. Motoba

*Laboratory of Physics, Osaka Electro-Comm. University, Neyagawa 572-8530, Japan*

Th. A. Rijken

*Institute for Theoretical Physics, University of Nijmegen, Nijmegen, The Netherlands*

M. Kamimura

*Department of Physics, Kyushu University, 812-8581, Japan*

Detailed structure calculations in  ${}_{\Xi}^{12}\text{Be}$ ,  ${}_{\Xi}^5\text{H}$ ,  ${}_{\Xi}^9\text{Li}$ ,  ${}_{\Xi}^7\text{H}$  and  ${}_{\Xi}^{10}\text{Li}$  are performed within the framework of the microscopic two-, three- and four-body cluster models using the Gaussian Expansion Method. We adopted effective  $\Xi N$  interactions derived from the Nijmegen interaction models, which give rise to substantially attractive  $\Xi$ -nucleus potentials in accordance with the experimental indications.  ${}_{\Xi}^7\text{H}$  and  ${}_{\Xi}^{10}\text{Li}$  are predicted to have bound states. We propose to observe the bound states in future ( $K^-$ ,  $K^+$ ) experiments using  ${}^7\text{Li}$  and  ${}^{10}\text{B}$  targets in addition to the standard  ${}^{12}\text{C}$  target. The experimental confirmation of these states will provide information on the spin- and isospin-averaged  $\Xi N$  interaction.

## I. INTRODUCTION

In studies of nuclear interactions, two-body scattering data are the primary input for characterizing interaction models. However,  $S = -1$  hyperon (Y)-nucleon (N) scattering data are very limited because of experimental issues. For  $S = -2$  interactions such as  $\Lambda\Lambda$  and  $\Xi N$ , there are currently no scattering data. Therefore, the existing  $YN$  and  $YY$  interaction models have a substantial degree of ambiguity. Some  $YN$  scattering experiments will be performed at the Japan Proton Accelerator Research Complex (J-PARC) in the near future. Even at this facility, however, the possibility of performing  $\Xi N$  or  $\Lambda\Lambda$  scattering experiments is very limited or practically impossible. Hence, in order to obtain useful information on  $S = -2$  interactions, studies of many-body, hypernuclear structure are indispensable.

Our intention in this work is to investigate the possible existence of  $\Xi$  hypernuclei and to explore the properties of the underlying  $\Xi N$  interactions. Identification of  $\Xi$  hypernuclei in coming experiments at J-PARC will contribute significantly to understanding nuclear structure and interactions in  $S = -2$  systems, which can lead to an entrance into the world of multi-strangeness. In order to encourage new experiments seeking  $\Xi$  hypernuclei, it is essential to make a detailed theoretical investigation of the possible existence of bound states, despite some uncertainty in contemporary  $\Xi N$  interaction models.

We investigate here the binding energies and structure of  $\Xi$  hypernuclei produced by ( $K^-$ ,  $K^+$ ) reactions on light targets on the basis of microscopic cluster mod-

els. One of the primary issues is how to choose the  $\Xi N$  interaction. Although there are no definitive data for any  $\Xi$  hypernucleus at present, a few experimental data indicate that  $\Xi$ -nucleus interactions are attractive. One example is the observed spectrum of the ( $K^-$ ,  $K^+$ ) reaction on a  ${}^{12}\text{C}$  target, where the cross sections for  $\Xi^-$  production in the threshold region can be interpreted by assuming a  $\Xi$ -nucleus Wood-Saxon (WS) potential with a depth of  $\sim 14$  MeV [1]. Other indications of attractive  $\Xi$ -nucleus interactions are given by certain emulsion data, the events for twin- $\Lambda$  hypernuclei, where the initial  $\Xi^-$  energies were determined by the identification of all fragments after the  $\Xi^- p\text{-}\Lambda\Lambda$  conversion in nuclei. The inferred  $\Xi^-$  binding energies are substantially larger than those obtained using only the Coulomb interaction [2]. When these  $\Xi^-$  states are assumed to be  $1p$  states, the WS potentials obtained from the binding energies are similar to the one above. These data suggest that the average  $\Xi N$  interaction should be attractive, which we utilize to select the appropriate interaction models. In this work we adopt two types of  $\Xi N$  interactions, the Nijmegen Hard-Core model D (ND) [3] and the Extended Soft-Core model (ESC04) [4, 5].

The structure of light  $p$ -shell nuclei can be reasonably described in terms of cluster models composed of two- or three-body subunits. Here, we model the possible  $\Xi^-$  hypernuclei produced by ( $K^-$ ,  $K^+$ ) reactions on available light  $p$ -shell targets as four-body cluster structures: The possible targets  ${}^{12}\text{C}$ ,  ${}^{11}\text{B}$ ,  ${}^{10}\text{B}$ ,  ${}^9\text{Be}$  and  ${}^7\text{Li}$  naturally lead to such cluster configurations as  $\alpha\alpha t\Xi^-({}_{\Xi}^{12}\text{Be})$ ,  $\alpha\alpha 2n\Xi^-({}_{\Xi}^{11}\text{Li})$ ,  $\alpha\alpha n\Xi^-({}_{\Xi}^{10}\text{Li})$ ,

$\alpha t n \Xi^-$  ( ${}_{\Xi^-}^9\text{He}$ ) and  $\alpha n n \Xi^-$  ( ${}_{\Xi^-}^7\text{H}$ ), respectively, by conversion of a proton into a  $\Xi^-$ . (In our model calculations, the  $\alpha \Xi^-$  potential is generated from a G-matrix  $\Xi N$  interaction via a folding procedure.) Here, among the above  $\Xi^-$  hypernuclei,  ${}_{\Xi^-}^7\text{H}(\alpha n n \Xi^-)$  is the lightest  $\Xi^-$  bound system, as shown in the following section. In the case of lighter targets,  ${}^6\text{Li}$ ,  ${}^4\text{He}$ ,  ${}^3\text{He}$  and  $d$ , the  $\Xi^-$ -hypernuclear states are composed of  $\alpha n \Xi^-$ ,  $p n n \Xi^-$  ( $t \Xi^-$ ),  $p n \Xi^-$  and  $n \Xi^-$  configurations, respectively. However, these systems are not expected to support bound states, considering the weakly attractive nature of the  $\Xi N$  interactions suggested so far, except for Coulomb-bound (atomic) states. Thus, possible  $\Xi^-$  hypernuclear states to be investigated lie in the light  $p$ -shell region and may be considered to have basically a four-body cluster structure.

This paper is organized as follows: In Sec.II, we describe the basic properties of the  $\Xi N$  interaction models and make clear what is relevant in the present four-body calculations. In Sec.III, we perform the calculation of  ${}_{\Xi^-}^{12}\text{Be}(\alpha \alpha t \Xi^-)$  with some approximations, in order to fix the  $\Xi N$  interaction strengths to be consistent with the ( $K^-$ ,  $K^+$ ) data. The four-body cluster models, based on the Gaussian Expansion Method (GEM), have been developed in a series of works for  $\Lambda$  and double- $\Lambda$  hypernuclei [6, 7, 8, 9, 10, 11, 12]. In this work, similar cluster models are applied to  ${}_{\Xi^-}^{12}\text{Be}(\alpha \alpha t \Xi^-)$ ,  ${}_{\Xi^-}^7\text{H}(\alpha n n \Xi^-)$  and  ${}_{\Xi^-}^{10}\text{Li}(\alpha \alpha n \Xi^-)$ . In Sec.IV, first we show the calculated behavior of the  ${}_{\Xi^-}^5\text{H}(\alpha \Xi^-)$  and  ${}_{\Xi^-}^9\text{Li}(\alpha \alpha \Xi^-)$  systems, as a function of the  $k_F$  parameter in the  $\Xi N$  G-matrix interaction, to confirm the binding mechanism before adding neutron(s). Then, in Sec.V we discuss the calculated results for  ${}_{\Xi^-}^7\text{H}(\alpha n n \Xi^-)$  and  ${}_{\Xi^-}^{10}\text{Li}(\alpha \alpha n \Xi^-)$ .

## II. $\Xi N$ INTERACTIONS

As stated above, the experimental information on  $\Xi N$  interactions is quite uncertain. It should be complemented by theoretical considerations. Various  $SU_3$ -based interaction models have been proposed so far. In the construction of these models, the scarce  $YN$  scattering data are supplemented by the rich  $NN$  scattering data through use of  $SU_3$  relations among the meson-baryon coupling constants. Though these models are more or less similar in  $S = -1$  systems, their  $S = -2$   $\Xi N$  predictions differ dramatically from one another; most are repulsive on average. In order to generate an attractive  $\Xi N$  interaction on the basis of OBE modeling, it seems to be necessary that specific features are imposed. In the past, the ND model has been popular for  $S = -2$  interactions, because this model is compatible with the strong  $\Lambda\Lambda$  attraction indicated by the older data on double  $\Lambda$  hypernuclei, and also it yields attractive  $\Xi$ -nucleus interactions. These aspects of ND are the result of its specific feature that the unitary-singlet scalar meson is included without any scalar-octet mesons. In this case, the strong  $\Xi N$  attraction originates from this scalar-singlet meson which gives the same contributions in all  $YN$  and  $YY$

channels. In the case of other Nijmegen OBE models, the attractive contributions of the scalar-singlet mesons are substantially cancelled by those of the scalar-octet mesons, and their  $\Xi N$  sectors are repulsive on average. A different OBE modeling for attractive  $\Xi N$  interactions has been adopted in the Ehime model [14], where the insufficient  $\Xi N$  attraction given by scalar-nonet mesons is supplemented by adding another scalar-singlet meson  $\sigma$  and the coupling constant  $g_{\Xi\Xi\sigma}$  is adjusted so as to give reasonable  $\Xi N$  attraction, independent of the SU3-relations among coupling constants. The two models, ND and Ehime, are essentially similar, in that substantial parts of the  $\Xi N$  attraction result from the scalar-singlet mesons.

More recently, new interaction models ESC04 (a,b,c,d) have been introduced, models in which two-meson and meson-pair exchanges are taken into account, and in principle no *ad hoc* effective boson-exchange potentials are included [4, 5]. The features of the ESC04 models differ significantly from those of the OBE models, especially in the  $S = -2$  channels. Among the ESC04 models, ESC04d is distinguished, because the resulting  $\Xi$ -nucleus interaction gives attraction suggested by the above experimental situation. This is mainly due to the following mechanism: A remarkably strong attraction appears in the  $T = 0$  triplet-even ( ${}^{13}S_1$ ) state, because the strongly repulsive contribution of vector mesons is cancelled by the attractive contributions from axial-vector mesons. In fact, the attraction in this state is so strong that peculiar  $\Xi$  bound states are produced in few-body systems [13], though such considerations lie outside the scope of the work presented in this paper. In later calculations, the important points are the spin- and isospin-averaged even-state interactions, which are strongly attractive owing to the significant  ${}^{13}S_1$ -state attraction. Another important feature of ESC04d in the  $S = -2$  channel is that the meson-pair exchange terms give rise to strong  $\Lambda\Lambda$ - $\Xi N$ - $\Sigma\Sigma$  and  $\Xi N$ - $\Lambda\Sigma$ - $\Sigma\Sigma$  coupling interactions. This feature of ESC04d makes the conversion widths of  $\Xi$ -hypernuclear states far larger than those for ND.

TABLE I: Partial wave contributions to  $U_{\Xi}(\rho_0)$ . In the case of ESC04d, the medium-induced repulsion is included by taking  $\alpha_V = 0.18$ . In the case of ND, the hard-core radii are taken as  $r_c = 0.52$  and  $0.45$  fm in the  ${}^{11}S_0$  and the other states, respectively.

model	$T$	${}^1S_0$	${}^3S_1$	${}^1P_1$	${}^3P_0$	${}^3P_1$	${}^3P_2$	$U_{\Xi}$	$\Gamma_{\Xi}$
ESC04d	0	6.3	-18.4	1.2	1.5	-1.3	-1.9		
	1	7.2	-1.7	-0.8	-0.5	-1.2	-2.5	-12.1	12.7
ND	0	-3.0	-0.5	-2.1	-0.2	-0.7	-1.9		
	1	-4.1	-4.2	-3.0	-0.0	-3.1	-6.5	-29.5	0.8

Our cluster models are composed of cluster units ( $\alpha$  and  $t$ ),  $n$  and  $\Xi^-$ , where the  $\alpha(t)\Xi^-$  interactions are obtained by folding the  $\Xi N$  G-matrix interactions into the density of  $\alpha(t)$ . According to the method described in Refs. [4, 5], the  $\Xi N$  G-matrix interactions are derived

from ESC04d and ND in nuclear matter, where the imaginary parts arise from the energy-conserving transitions from  $\Xi N$  to  $\Lambda\Lambda$  channels in the nuclear medium. The resulting complex G-matrix interactions are represented as  $k_F$ -dependent local potentials

$$G_{TS}^{(\pm)}(r, k_F) = \sum_{i=1}^3 (a_i + b_i k_F + c_i k_F^2) \exp(-r^2/\beta_i^2), \quad (2.1)$$

where  $k_F$  is the Fermi momentum of nuclear matter. The suffixes (+) and (-) specify even and odd, respectively. In our applications to finite  $\Xi$  systems, it is plausible to obtain the  $k_F$  values from the average density in the respective systems. In a similar G-matrix approach to  $\Lambda$  hypernuclei, for instance, the  $\Lambda N$  G-matrix interactions can be adopted to reproduce the observed  $\Lambda$  binding energy ( $B_\Lambda$ ) by choosing appropriate  $k_F$  values. Such a procedure cannot be applied strictly in the case of  $\Xi$  hypernuclei, because there exist no definitive experimental data. In this work, we are obliged to choose the  $k_F$  values rather arbitrarily but within a reasonable range ( $0.8 \sim 1.2 \text{ fm}^{-1}$  in light  $p$ -shell systems). Here, the experimental indication for the existence of  ${}_{\Xi}^{12}\text{Be}$  is used to adopt the  $\Xi N$  G-matrix interactions, although it is not so definite because an experimental  $\Xi$  binding energy ( $B_\Xi$ ) could not be extracted. As shown later, the adjustable parts included in ND and ESC04d are determined so that the  $\Xi$   $s$ -state energy in our model of  ${}_{\Xi}^{12}\text{Be}$  has the value  $-2.2 \text{ MeV}$  for an adequate value of  $k_F$ , being obtained from the  $\Xi$ -nucleus WS potential with the depth  $-14 \text{ MeV}$  [1] where the Coulomb interaction is switched off. In the case of ND, this constraint can be realized by choosing the hard-core radius  $r_c$ : We take  $r_c = 0.52$  and  $0.45 \text{ fm}$  in the  ${}^{11}S_0$  state and the other states, respectively. The former choice is made so that the derived  ${}^{11}S_0$   $\Lambda\Lambda$  G-matrix interaction reproduces the  $\Lambda\Lambda$  bond energy observed in the double- $\Lambda$  hypernucleus. On the other hand, the constraint in the case of ESC04d is enforced by changing the parameter  $\alpha_V$  controlling the medium-induced repulsion [4]: We take  $\alpha_V = 0.18$ . Hereafter, ESC04d with  $\alpha_V = 0.18$  is denoted as ESC for simplicity.

In the Table I, we show the partial-wave contributions of the resulting  $\Xi$  potential depth  $U_\Xi$  in nuclear matter at normal density  $\rho_0$  ( $k_F = 1.35 \text{ fm}^{-1}$ ). The  $U_\Xi$  values are found to be very different for ESC and ND, because the odd-state contributions in the former are far more attractive than those in the latter. It is noted, however, the odd-state interactions play minor roles in light systems considered in this work. More important is that the spin- and isospin-dependence differs significantly between ESC and ND.

The interaction parameters ( $a_i$ ,  $b_i$  and  $c_i$ ) in our G-matrix interactions (2.1) are tabulated in Tables II and III for ESC and ND, respectively. Hereafter, G-matrix interactions derived from ESC and ND are denoted as  $G_{ESC}$  and  $G_{ND}$ , respectively.

The features of our G-matrix interactions can be

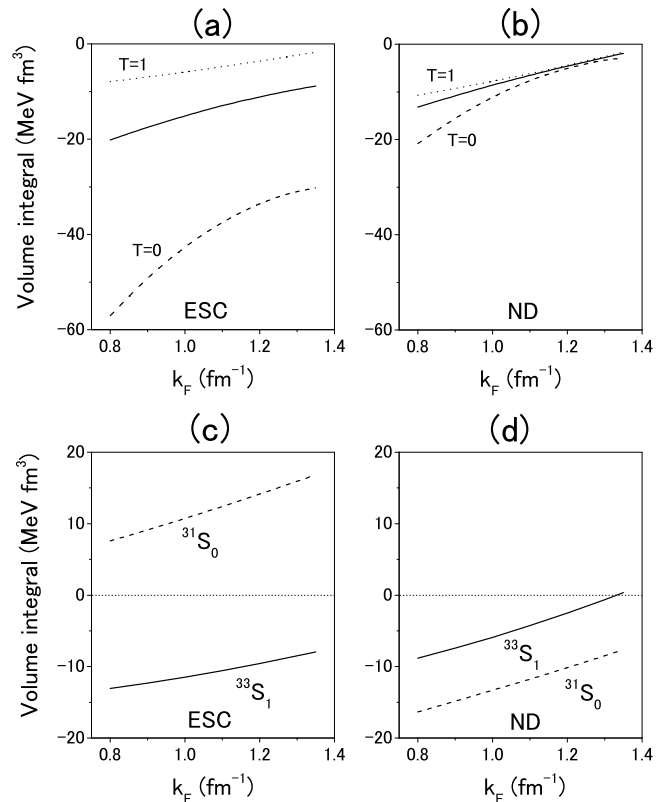


FIG. 1: The volume integrals of  $\bar{G}^{(+)} = (G_{00}^{(+)} + 3G_{01}^{(+)} + 3G_{10}^{(+)} + 9G_{11}^{(+)})/16$  are drawn as a function of  $k_F$  by solid curves in (a) for ESC and in (b) for ND. Here,  $T = 0$  (dashed) and  $T = 1$  (dotted) parts show the volume integrals of  $(G_{00}^{(+)} + 3G_{01}^{(+)})/4$  and  $(G_{10}^{(+)} + 3G_{11}^{(+)})/4$ , respectively. In (c), the volume integrals of  ${}^{33}S_1$  and  ${}^{31}S_0$  components for ESC are drawn by solid and dashed curves, respectively. The corresponding ones for ND are in (d).

demonstrated clearly by the volume integrals of the G-matrix interaction:  $J_V(k_F) = \int_0^\infty G(r, k_F) r^2 dr$ . Here, we define the spin- and isospin-averaged interactions as  $\bar{G}^{(\pm)} = (G_{00}^{(\pm)} + 3G_{01}^{(\pm)} + 3G_{10}^{(\pm)} + 9G_{11}^{(\pm)})/16$ . The volume integrals of  $\bar{G}^{(+)}(r, k_F)$  are drawn as a function of  $k_F$  in Fig. 1, where (a) and (b) are for ESC and ND, respectively. It should be noted here that the even-state interaction of ESC is more attractive than that of ND. In the cases of our cluster systems,  $\Xi$ -states are determined dominantly by  $\alpha$   $\Xi$  folding interactions derived from  $\bar{G}^{(\pm)}(r, k_F)$ . The  $\bar{G}^{(-)}$  for ND is far more attractive than that for ESC, though their contributions in  $s$ -shell systems are very small. Similarly, (c) and (d) in Fig. 1 show the volume integrals of the triplet- and singlet-even state interactions in the  $T = 1$  state for ESC and ND, respectively. Here, the  ${}^{33}S_1$  and  ${}^{31}S_0$  interactions in ESC are found to be attractive and repulsive, respectively. On the other hand, both of  ${}^{33}S_1$  and  ${}^{31}S_0$  interactions are attractive in ND, and the latter is more attractive than the former. Namely, the  $T = 1$  spin-spin interaction in ND (ESC) is repulsive (attractive). This difference of the

$T = 1$  spin-spin interactions for ESC and ND is reflected in the level structures of  ${}_{\Xi}^7\text{H}$  and  ${}_{\Xi}^{10}\text{Li}$ , as shown later.

Another important difference between ESC and ND is that the  $\Lambda\Lambda$ - $\Xi N$ - $\Sigma\Sigma$  coupling interaction in the former is far stronger than that in the latter. This is reflected by the fact that the calculated value of the conversion width  $\Gamma_{\Xi}$  for ESC is far larger than that for ND, as exhibited in Table I.

TABLE II: The parameters in the G-matrix interaction  $G_{TS}^{(\pm)}(r, k_F)$  given by (2.1) for ESC. Entries are given in units of  $a$  [MeV],  $b$  [MeV·fm] and  $c$  [MeV·fm<sup>2</sup>]

	$\beta_i$ (fm)	0.50	0.90	2.00
$G_{00}^{(+)}$	$a$	0.0	-690.8-309.0 <i>i</i>	-2.759
	$b$	0.0	1263.+252.4 <i>i</i>	0.0
	$c$	0.0	-451.7-111.0 <i>i</i>	0.0
$G_{01}^{(+)}$	$a$	-6959.	756.5	-1.317
	$b$	11280.	-1567.	0.0
	$c$	-4371.	627.2	0.0
$G_{00}^{(-)}$	$a$	-1634.	257.8	-1.528
	$b$	3426.	-137.4	0.0
	$c$	-965.8	60.78	0.0
$G_{01}^{(-)}$	$a$	-5692.	175.0-15.50 <i>i</i>	-1.411
	$b$	7697.	-583.9+24.31 <i>i</i>	0.0
	$c$	-2667.	303.8-13.91 <i>i</i>	0.0
$G_{10}^{(+)}$	$a$	-216.4	48.96	-1.838
	$b$	676.0	-83.76	0.0
	$c$	-198.1	43.36	0.0
$G_{11}^{(+)}$	$a$	527.9	-121.8	-1.787
	$b$	85.16	-10.83	0.0
	$c$	13.25	9.351	0.0
$G_{10}^{(-)}$	$a$	-2671.	36.08	-1.043
	$b$	3343.	-116.6	0.0
	$c$	-1034.	53.97	0.0
$G_{11}^{(-)}$	$a$	1435.	-166.3	-1.168
	$b$	451.1	-24.19	0.0
	$c$	-131.2	18.44	0.0

Our cluster models for  $A = 7$  and 10 systems are composed of  $\alpha nn\Xi^-$  and  $\alpha\alpha n\Xi^-$ , respectively, where the  $\Xi N$  G-matrix interactions are used to obtain  $\alpha\Xi^-$  folding potentials based on the  $(0s_{1/2})^4$  configuration with  $b_N = 1.358$  fm. It is problematic, on the other hand, to use the G-matrix interactions for the  $\Xi n$  parts. The reason is as follows: Correlations of  $\Xi n$  pairs are treated exactly in our model space spanned by Gaussian functions, which means some double counting for  $\Xi n$  short-range correlations that has been already included in the G-matrix interactions. Though a reasonable way out of this problem is to use directly the bare potentials (ESC and ND), there appear some difficulties in such treatments: In the case of ESC, the  $\Xi N$ - $\Lambda\Sigma$  and  $\Xi N$ - $\Lambda\Sigma$ - $\Sigma\Sigma$  coupling potentials in the  $T = 1$  channels make our

TABLE III: The parameters in the G-matrix interaction  $G_{TS}^{(\pm)}(r, k_F)$  given by (2.1) for ND. Entries are given in units of  $a$  [MeV],  $b$  [MeV·fm] and  $c$  [MeV·fm<sup>2</sup>]

	$\beta_i$ (fm)	0.50	0.90	2.00
$G_{00}^{(+)}$	$a$	-8769.	456.1-102.1 <i>i</i>	-2.505
	$b$	15530.	-1082.+91.45 <i>i</i>	0.0
	$c$	-6383.	473.2-18.03 <i>i</i>	0.0
$G_{01}^{(+)}$	$a$	452.4	-105.8	-0.6861
	$b$	-25.82	10.75	0.0
	$c$	67.40	10.22	0.0
$G_{00}^{(-)}$	$a$	-7382.	-168.9	-3.141
	$b$	8672.	-140.1	0.0
	$c$	-3145.	69.22	0.0
$G_{01}^{(-)}$	$a$	-569.3	-231.1-7.788 <i>i</i>	0.0300
	$b$	2072.	-32.47+6.124 <i>i</i>	0.0
	$c$	-696.8	22.21-.5631 <i>i</i>	0.0
$G_{10}^{(+)}$	$a$	356.9	-138.5	-.3949
	$b$	110.3	13.97	0.0
	$c$	-1.818	7.792	0.0
$G_{11}^{(+)}$	$a$	436.0	-108.4	-1.334
	$b$	6.513	10.11	0.0
	$c$	46.10	10.88	0.0
$G_{10}^{(-)}$	$a$	75.12	-254.3	.1086
	$b$	939.6	-.0260	0.0
	$c$	-269.5	7.792	0.0
$G_{11}^{(-)}$	$a$	-281.0	-218.5	-1.003
	$b$	1227.	-5.773	0.0
	$c$	-422.7	11.82	0.0

treatment extremely complicated. In the case of ND, although these coupling potentials are not taken into account, the hard-core singularities cannot be treated in our Gaussian model space. Thus, we adopt here simple three-range Gaussian substitutes simulating the bare potentials. They are fitted so that the G-matrices derived from them simulate the original  $T = 1$  G-matrices at  $k_F = 1.0$  fm<sup>-1</sup>. Here, the  $\Xi N$ - $\Lambda\Sigma$  and  $\Xi N$ - $\Lambda\Sigma$ - $\Sigma\Sigma$  couplings in the ESC case are effectively renormalized into the  $\Xi N$  single-channel potentials. The determined interaction parameters are given in Table IV for ESC and ND.

### III. ${}_{\Xi}^{12}\text{Be}(\alpha\alpha t\Xi^-)$ SYSTEM

Let us start from the analysis for the  ${}_{\Xi}^{12}\text{Be}$  ( ${}^{11}\text{B} + \Xi^-$ ) hypernucleus produced by the  ${}^{12}\text{C}(K^-, K^+)$  reaction, adopting the  $\alpha\alpha t\Xi^-$  four-body model. In this case, the  $(T, J^\pi) = (1, 1^-)$  states are produced, because the  $T_z$  component is transformed by  $\Delta T_z = 1$  on the  $T = 0$  target. This system is important in a double sense. One is that in BNL-E885 a fairly deep  ${}^{11}\text{B}-\Xi^-$  potential was in-

TABLE IV: Parameters of the three-range Gaussian interactions simulating (a) ESC and (b) ND in the  $T = 1 \Xi n$  states.

(a) ESC			
$\beta_i$ (fm)	0.40	0.80	1.50
$^{31}E$	519.5	66.27	-7.230
$^{33}E$	217.4	-170.0	-7.058
$^{31}O$	0.0	-39.56	-5.178
$^{33}O$	0.0	-55.40	-6.936
(b) ND			
$\beta_i$ (fm)	0.50	0.90	2.00
$^{31}E$	1076.	-159.6	-5.432
$^{33}E$	1331.	-134.0	-7.610
$^{31}O$	0.0	-32.30	-5.432
$^{33}O$	0.0	18.16	-7.610

indicated as mentioned in the previous section. The other is that this reaction is planned as the Day-1 experiment at J-PARC.

The above-mentioned G-matrix interactions  $G_{ESC}$  and  $G_{ND}$  are adjusted so as to be consistent with the Woods-Saxon potential depth of BNL-E885 within the framework of the  $\alpha\alpha t \Xi^-$  four-body model.

### A. Model and Interaction

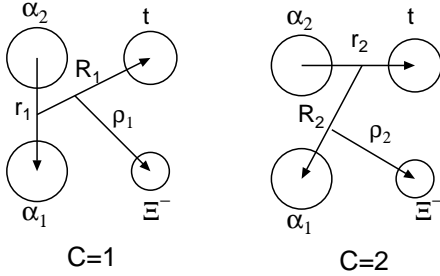


FIG. 2: Jacobian coordinates for the  $\alpha\alpha t \Xi^-$  ( $^{12}\Xi^- \text{Be}$ ) four-body system. The two  $\alpha$  clusters are to be symmetrized.

In the case of an  $\alpha\alpha t \Xi^-$  four-body model, we take two sets of Jacobian coordinates as shown in Fig. 2, since we get sufficiently converged energies using only those two sets of Jacobian coordinates. The total Hamiltonian and the Schrödinger equation are given by

$$(H - E) \Psi_{JM}(\Xi^- \text{Be}) = 0, \quad (3.1)$$

$$H = T + \sum_{a,b} V_{ab} + V_{\text{Pauli}}, \quad (3.2)$$

where  $T$  is the kinetic-energy operator and  $V_{ab}$  is the interaction between constituent particles  $a$  and  $b$ . The OCM projection operator  $V_{\text{Pauli}}$  will be given below. The total wavefunction is described as a sum of amplitudes of the rearrangement channels ( $c = 1$  and  $2$ ) of Fig. 2 in the  $LS$  coupling scheme:

$$\begin{aligned} \Psi_{JM, TT_z} (\Xi^- \text{Be}) &= \sum_{c=1}^2 \sum_{n, N, \nu, l, L, \lambda} \sum_{S, I, K} C_{nlNL\nu\lambda SIK}^{(c)} \\ &\times \mathcal{S}_\alpha \left[ \Phi(\alpha_1) \Phi(\alpha_2) \left[ \Phi_{\frac{1}{2}}(t) \chi_{\frac{1}{2}}(\Xi^-) \right]_S \right. \\ &\times \left. \left[ \left[ \phi_{nl}^{(c)}(\mathbf{r}_c) \psi_{NL}^{(c)}(\mathbf{R}_c) \right]_I \xi_{\nu\lambda}^{(c)}(\boldsymbol{\rho}_c) \right]_K \right]_{JM} \\ &\times \left[ \eta_{\frac{1}{2}}(t) \eta_{\frac{1}{2}}(\Xi^-) \right]_{T, T_z}. \end{aligned} \quad (3.3)$$

Here the operator  $\mathcal{S}_\alpha$  stands for the symmetrization operator for exchange of two  $\alpha$  clusters.  $\chi_{\frac{1}{2}}(\Xi^-)$  is the spin function of the  $\Xi^-$  particle and  $\eta_{\frac{1}{2}}(\Xi^-)$  is the isospin function of the  $\Xi^-$  particle. Following the Gaussian Expansion Method (GEM) [15, 16, 17], we take the functional form of  $\phi_{nlm}(\mathbf{r})$ ,  $\psi_{NLM}(\mathbf{R})$  and  $\xi_{\nu\lambda\mu}^{(c)}(\boldsymbol{\rho}_c)$  as

$$\begin{aligned} \phi_{nlm}(\mathbf{r}) &= r^l e^{-(r/r_n)^2} Y_{lm}(\hat{\mathbf{r}}), \\ \psi_{NLM}(\mathbf{R}) &= R^L e^{-(R/R_N)^2} Y_{LM}(\hat{\mathbf{R}}), \\ \xi_{\nu\lambda\mu}(\boldsymbol{\rho}) &= \rho^\lambda e^{-(\rho/\rho_\nu)^2} Y_{\lambda\mu}(\hat{\boldsymbol{\rho}}), \end{aligned} \quad (3.4)$$

where the Gaussian range parameters are chosen according to geometrical progressions:

$$\begin{aligned} r_n &= r_1 a^{n-1} \quad (n = 1 - n_{\text{max}}), \\ R_N &= R_1 A^{N-1} \quad (N = 1 - N_{\text{max}}), \\ \rho_\nu &= \rho_1 \alpha^{\nu-1} \quad (\nu = 1 - \nu_{\text{max}}). \end{aligned} \quad (3.5)$$

The eigenenergy  $E$  in Eq.(3.1) and the coefficients  $C$  in Eq.(3.3) are to be determined by the Rayleigh-Ritz variational method.

As for the  $\alpha\alpha$  and  $\alpha t$  interactions, we employ the potentials which have been used often in the OCM-based cluster-model study of light nuclei: Our potentials  $V_{\alpha\alpha}$  [18] and  $V_{\alpha t}$  [19] reproduce reasonably well the low-lying bound states and low-energy scattering phase shifts of the  $\alpha\alpha$  and  $\alpha t$  systems, respectively. The Coulomb potentials are constructed by folding the  $p$ - $p$  Coulomb force into the proton densities of all the participating clusters.

The Pauli principle between nucleons belonging to  $\alpha$  and  $x (= \alpha, t)$  clusters is taken into account by the orthogonality condition model (OCM) [20]. The OCM projection operator  $V_{\text{Pauli}}$  appearing in Eq. (3.2) is represented by

$$V_{\text{Pauli}} = \lim_{\gamma \rightarrow \infty} \gamma \sum_f |\phi_f(\mathbf{r}_{\alpha x})\rangle \langle \phi_f(\mathbf{r}'_{\alpha x})|, \quad (3.6)$$

which rules out the amplitude of the Pauli-forbidden  $\alpha - x$  relative states  $\phi_f(\mathbf{r}_{\alpha x})$  from the four-body total wavefunction [21]. The forbidden states are  $f =$

$0S, 1S, 0P, 0D$  for  $x = t$  and  $f = 0S, 1S, 0D$  for  $x = \alpha$ . The Gaussian range parameter  $b$  of the single-particle  $0s$  orbit in the  $\alpha$  particle  $(0s)^4$  is taken to be  $b = 1.358$  fm so as to reproduce the size of the  $\alpha$  particle. For simplicity the same size is assumed for the  $t$  cluster in treating the Pauli principle. In the actual calculations, the strength  $\gamma$  for  $V_{\text{Pauli}}$  is taken to be  $10^4$  MeV, which is large enough to push the unphysical forbidden state to the very high energy region, while keeping the physical states unchanged.

Using the  $V_{\alpha\alpha}$  and  $V_{\alpha t}$  potentials, we perform the three-body calculation for the  $^{11}\text{B}(\alpha\alpha t)$  system. The calculated values of the ground ( $3/2_1^-$ ) and the first excited ( $1/2_1^-$ ) states in  $^{11}\text{B}$  are overbound in comparison with the experimental values. In order to put the subsequent four-body calculations for  $^{12}_{\Xi^-}\text{Be}(\alpha\alpha t\Xi^-)$  on a sound basis, we introduce a phenomenological  $\alpha\alpha t$  three-body force of the following form:

$$V_{\alpha\alpha t} = v_0 \exp[-(r_{\alpha_1 t}/\beta)^2 - (r_{\alpha_2 t}/\beta)^2]. \quad (3.7)$$

Here we adopt  $v_0 = +95$  MeV and  $\beta = 2.26$  fm in order to reproduce the  $^{11}\text{B}(3/2_1^-)$  ground state energy. For the excitation energy of the  $^{11}\text{B}(1/2_1^-)$  state, we stick to the exact experimental value instead of the calculated value, when we perform the hypernuclear four-body calculations.

### B. Results for $^{12}_{\Xi^-}\text{Be}$ and the appropriate $k_F$ parameter

As mentioned before, our  $\Xi N$  interactions are adjusted so as to give the  $\Xi^-$   $s$ -state energy  $-2.2$  MeV in the  $^{12}_{\Xi^-}\text{Be}$  system. This value is consistent with the observed spectrum of the  $^{12}\text{C}(K^-, K^+)$  reaction which suggests the WS potential depth of 14 MeV [1]. If we assume spin-nonflip dominance for the  $^{12}\text{C}(K^-, K^+)$  reaction, the  $[p_{3/2}^{-1} s_{1/2}^{\Xi^-}]_{J=1^-}$  state is naturally excited. Therefore, within the framework of the  $\alpha\alpha t\Xi^-$  four-body model, the  $k_F$  parameters in the  $\alpha\Xi^-$  and  $t\Xi^-$  potentials, without Coulomb interaction, are tuned so that the  $1_1^-$  state energies agree with  $-2.2$  MeV. We listed in Table V, the calculated  $\Xi^-$ -binding energies ( $B_{\Xi^-}$ ) of the  $1_1^-$  and  $2_1^-$  states. In the case of  $G_{\text{ESC}}$ , the  $2_1^-$  state is obtained at a lower energy than the  $1_1^-$  state. On the other hand, the use of  $G_{\text{ND}}$  leads to the opposite order. In our model, this is because  $^{33}\text{S}_1$  interaction for ESC(ND) is more(less) attractive than the  $^{31}\text{S}_0$  interaction as shown in Fig.1(c) and (d). The contribution of the  $\Xi^- \alpha$  and  $\Xi^- t$  Coulomb forces amounts to about 1.5 MeV. The conversion widths obtained from the imaginary part of  $G_{\text{ESC}}$  is far larger than that for  $G_{\text{ND}}$ . This is because the  $^1\text{S}_0$   $\Lambda\Lambda$ - $\Xi N$ - $\Sigma\Sigma$  coupling interaction in ESC is far stronger than that in ND.

We found the appropriate  $k_F$  parameter values of the effective  $\Xi N$  interactions to be  $k_F = 1.055$  fm $^{-1}$  (ESC) and  $k_F = 1.025$  fm $^{-1}$ (ND), which are consistent with

the experimental indication in  $^{12}_{\Xi^-}\text{Be}$ . These interactions provide our basis to investigate the  $A = 7$  and  $10$   $\Xi^-$  hypernuclei.

## IV. RESULTS FOR TYPICAL SYSTEMS COMPOSED OF $\alpha\Xi^-$ ( ${}_{\Xi^-}^5\text{H}$ ) AND $\alpha\alpha\Xi^-$ ( ${}_{\Xi^-}^9\text{Li}$ )

Let us study the  $\alpha\Xi^-$  and  $\alpha\alpha\Xi^-$  systems in order to demonstrate the basic features of the  $\alpha\Xi^-$  interactions. In the cases of  ${}_{\Xi^-}^7\text{H}(\alpha nn\Xi^-)$  and  ${}_{\Xi^-}^{10}\text{Li}(\alpha\alpha n\Xi^-)$ , the dominant parts of the  $\Xi^-$  binding energies are given by the  $\alpha\Xi^-$  interactions because of the weak binding of the additional neutrons. The  $\alpha\Xi^-$  interaction is derived by folding the  $\Xi N$  G-matrix interaction into the wave function of the  $\alpha$ . The spin- and isospin-dependent parts, being remarkably different between ESC and ND, vanish in a folding procedure involving a spin- and isospin-saturated system such as the  $\alpha$ . Thus, the  $\alpha\Xi^-$  interaction is determined only by the spin- and isospin-averaged  $\Xi N$  interaction  $\bar{G}^{(\pm)}(r; k_F)$ , where the contribution of odd-state part  $\bar{G}^{(-)}$  is quite small in the two-body  $\alpha\Xi^-$  system. It should be stressed that  $\alpha$ -cluster systems such as  $\alpha\Xi^-$  and  $\alpha\alpha\Xi^-$  give the most basic information on the spin- and isospin-averaged parts of  $\Xi N$  interactions. These parts correspond to so-called spin-independent parts in interactions represented by the  $(\sigma\sigma)$ ,  $(\tau\tau)$  and  $(\sigma\sigma)(\tau\tau)$  operators.

Here, it is of vital importance how one chooses the  $k_F$  parameters in our G-matrix interactions. The parameter  $k_F$  specifies the nuclear matter density in which the G-matrix interactions are constructed. It is most plausible that a corresponding value in a finite system is obtained from an average density. Our basic interactions (ESC and ND) are adjusted so that the derived G-matrix interactions give rise to reasonable  $\Xi^-$  binding in an  $A \sim 12$  system for  $k_F = 1.0 \sim 1.1$  fm $^{-1}$  adequately chosen. Considering that the suitable values  $k_F = 1.055$  fm $^{-1}$ (ESC) and  $1.025$  fm $^{-1}$ (ND) for  $^{12}_{\Xi^-}\text{Be}$ , it is a modest change to take  $k_F = 0.9$  fm $^{-1}$  in the  $A = 4 \sim 6$  systems. In fact, we have had successful prior experience. In Ref.[7], we studied the structure of  ${}_{\Lambda}^5\text{He}$ ,  ${}_{\Lambda}^9\text{Be}$  and  ${}_{\Lambda}^{13}\text{C}$  using the  $\Lambda N$  G-matrix interactions, where consistent results were obtained by choosing the  $k_F$  parameters to be around  $0.9$  fm $^{-1}$  for  ${}_{\Lambda}^5\text{He}$  and  ${}_{\Lambda}^9\text{Be}$  and to be around  $1.1$  fm $^{-1}$  for  ${}_{\Lambda}^{13}\text{C}$ . Here, we take three values of  $k_F$  parameters for our  $\Xi N$  G-matrix interactions in order to study  $A = 7$  and  $A = 10$  systems:  $k_F=0.9, 1.055$  and  $1.3$  fm $^{-1}$  for ESC, and  $k_F=0.9, 1.025$  and  $1.3$  fm $^{-1}$  for ND. So, the  $k_F$  values for  $A = 10$  system are considered to be  $k_F \sim 1.0$  fm $^{-1}$ , while those for  $A = 6$  near  $k_F = 0.9$  fm $^{-1}$ . The unreasonably large value of  $k_F = 1.3$  fm $^{-1}$ , as a trial, is used only to demonstrate the  $k_F$  dependences of the results.

In Table VI, we show the calculated energies and r.m.s radii for the  $\alpha\Xi^-$  system for three  $k_F$  values of the  $\Xi N$  G-matrix interactions. Of course, Coulomb bound ( $\Xi^-$ -atomic) states are obtained, even if the strong inter-

TABLE V: The calculated  $B_{\Xi^-}$  (MeV) of the  $1_1^-$  and  $2_1^-$  states using ESC and ND potentials for  $^{12}_{\Xi^-}\text{Be}$ . In order to reproduce the 'observed'  $B_{\Xi^-}$ , we tuned  $k_F = 1.055(\text{fm}^{-1})$  and  $1.025(\text{fm}^{-1})$  for the ESC and ND potentials, respectively. The energies using the ESC and ND potentials without and with Coulomb potentials between  $\alpha$  and  $\Xi^-$  and between triton and  $\Xi^-$ , are listed respectively.

	ESC		ND	
	(without Coulomb)	(with Coulomb)	(without Coulomb)	(with Coulomb)
$1^- B_{\Xi^-}$ (MeV)	2.24	4.98	2.23	4.82
$\Gamma$ (MeV)	3.95	4.64	1.38	1.66
$2^- B_{\Xi^-}$ (MeV)	3.18	6.08	1.56	4.06
$\Gamma$ (MeV)	4.24	4.80	0.93	1.18

TABLE VI: The calculated energies of the  $1/2^+$  state,  $E$ , and r.m.s radii,  $r_{\alpha-\Xi^-}$ , in the  $\alpha\Xi^-$  ( ${}^5_{\Xi^-}\text{H}$ ) system for several values of  $k_F$ . The values in parentheses are energies when the imaginary part of the  $\alpha\Xi^-$  interactions are switched off. The energies are measured from the  $\alpha + \Xi^-$  threshold.

(a) $\alpha\Xi^-$ (ESC)				
with	$k_F$ ( $\text{fm}^{-1}$ )	0.9	1.055	1.3
Coulomb	$E$ (MeV)	-1.36	-0.26	-0.14
		(-1.71)	(-0.57)	(-0.19)
	$\Gamma$ (MeV)	2.64	0.86	0.15
	$r_{\alpha-\Xi^-}$ (fm)	3.89	6.83	13.6
without	$E$ (MeV)	unbound	unbound	unbound
Coulomb		(-0.64)		
	$\Gamma$ (MeV)	-	-	-
(b) $\alpha\Xi^-$ (ND)				
with	$k_F$ ( $\text{fm}^{-1}$ )	0.9	1.025	1.3
Coulomb	$E$ (MeV)	-0.57	-0.32	-0.15
		(-0.57)	(-0.32)	(-0.16)
	$\Gamma$ (MeV)	0.16	0.06	0.004
	$r_{\alpha-\Xi^-}$ (fm)	6.87	9.82	15.65
without	$E$ (MeV)	unbound	unbound	unbound
Coulomb	$\Gamma$ (MeV)	-	-	-

actions are switched off. If a bound state is obtained without the Coulomb interaction, this state is called a nuclear-bound state. When a nuclear-unbound state becomes bound with help of the attractive Coulomb interaction, such a state is called a Coulomb-assisted bound state. Table VI summarizes our results that in each case the lowest state is found to be a Coulomb-assisted bound state, namely there appears no nuclear-bound state. It is noted, in this Table, that a nuclear-bound state is obtained in the case of  $G_{ESC}(k_F = 0.9)$  if its imaginary part is switched off: Though the real part of the  $\alpha\Xi^-$  interaction for  $G_{ESC}(k_F = 0.9)$  is attractive enough to

give a nuclear-bound state, the strong imaginary part makes the resulting state nuclear-unbound. In any case, the spin- and isospin-averaged even-state part  $\tilde{G}^{(+)}$  for  $G_{ESC}$  is far more attractive than the corresponding part of  $G_{ND}$ .

In Table VII, we list the calculated results for the  $\alpha\alpha\Xi^-$  system. It should be noted, here, that nuclear-bound states are obtained in both cases of  $G_{ESC}$  and  $G_{ND}$  unless an unreasonably large value of  $k_F$  is chosen. The calculated energies for  $G_{ESC}$  are naturally larger than those for  $G_{ND}$ . In the  $\alpha\alpha\Xi^-$  system, however,  $\tilde{G}^{(-)}$  contributes significantly. It is remarked that the odd-state interaction in  $G_{ND}$  is far more attractive than that in  $G_{ESC}$ , which works to reduce the difference between both potentials in the  $\alpha\alpha\Xi^-$  system.

One notices in the Tables, that the decay widths for  $G_{ESC}$  are much larger than those for  $G_{ND}$ , when they are calculated for the same value of  $k_F$ . This is because the imaginary part of  $G_{ESC}$  is stronger than that of  $G_{ND}$ . The difference of the imaginary parts originates mainly from the different strengths of  ${}^{11}S_0 \Lambda\Lambda-\Xi N-\Sigma\Sigma$  coupling interactions in ESC and ND.

As mentioned before, noting that the choice of the  $k_F$  value  $\sim 0.9 \text{ fm}^{-1}(\alpha\Xi^-)$  and  $\sim 1.0 \text{ fm}^{-1}(\alpha\alpha\Xi^-)$ , are reasonable, respectively, we can expect the existence of nuclear-bound states, especially, in the latter case. Thus, we can say that observations of  $\alpha\Xi^-$  and  $\alpha\alpha\Xi^-$  systems certainly provide information about spin-independent parts of the  $\Xi N$  interactions. In reality, however, there are no corresponding nuclear targets to produce the above systems by the  $(K^-, K^+)$  reaction. As their actual substitutes, in the following, we investigate the structures of  ${}^7_{\Xi^-}\text{H}(\alpha nn\Xi^-)$  and  ${}^{10}_{\Xi^-}\text{Li}(\alpha\alpha n\Xi^-)$  having additional neutron(s), and propose to perform the  ${}^7\text{Li}(K^-, K^+)$  and  ${}^{10}\text{B}(K^-, K^+)$  reaction experiments with available targets.

## V. $A = 7$ AND $A = 10 \Xi^-$ HYPERNUCLEI

Here, we study  ${}^7_{\Xi^-}\text{H}$  and  ${}^{10}_{\Xi^-}\text{Li}$  on the basis of  $\alpha nn\Xi^-$  and  $\alpha\alpha n\Xi^-$  four-body cluster models, respectively. In

TABLE VII: The calculated energies of the  $1/2^+$  state,  $E$ , in the  $\alpha\alpha\Xi^-$  ( ${}_{\Xi}^9\text{Li}$ ) system for several values of  $k_F$ . The values in parentheses are energies when the imaginary part of the  $\alpha\Xi^-$  interaction are switched off. The energies are measured from the  $\alpha\alpha\Xi^-$  three-body breakup threshold.

(a) $\alpha\alpha\Xi^-$ (ESC)				
with	$k_F(\text{fm}^{-1})$	0.9	1.055	1.3
Coulomb	$E$ (MeV)	-4.81	-2.23	-0.83
		(-5.17)	(-2.57)	(-1.04)
	$\Gamma$ (MeV)	5.01	2.89	1.18
without	$E$ (MeV)	-2.54	-0.41	unbound
Coulomb		(-2.94)	(-0.77)	
	$\Gamma$ (MeV)	4.48	2.18	-

(b) $\alpha\alpha\Xi^-$ (ND)				
with	$k_F(\text{fm}^{-1})$	0.9	1.025	1.3
Coulomb	$E$ (MeV)	-2.87	-1.82	-0.79
		(-2.89)	(-1.83)	(-0.79)
	$\Gamma$ (MeV)	0.58	0.3	0.06
without	$E$ (MeV)	-1.02	-0.25	unbound
Coulomb		(-1.03)	(-0.26)	
	$\Gamma$ (MeV)	0.45	0.20	-

cluster-model studies, it is essential that interactions among cluster subunits be given consistently with respect to the corresponding threshold energies. Namely, low-energy bound-state energies and scattering phase shifts of  $\alpha n$ ,  $\alpha\alpha$ ,  $\alpha nn$ , and  $\alpha\alpha n$  subsystems should be reproduced reasonably by the corresponding interactions. We emphasize that these severe constraints are correctly satisfied in the present models, as mentioned below.

### A. Model and Interactions

For  ${}_{\Xi}^7\text{H}$  and  ${}_{\Xi}^{10}\text{Li}$ , all nine sets of the Jacobian coordinate of the four-body systems are shown in Fig. 3, respectively. The total Hamiltonian and the Schrödinger equation are given by

$$(H - E) \Psi_{JM}({}_{\Xi}^7\text{H}, {}_{\Xi}^{10}\text{Li}) = 0, \quad (5.1)$$

$$H = T + \sum_{a,b} V_{ab} + V_{\text{Pauli}}, \quad (5.2)$$

where  $T$  is the kinetic-energy operator,  $V_{ab}$  is the interaction between the constituent particle  $a$  and  $b$ , and the  $V_{\text{Pauli}}$  is the Pauli projection operator given by Eq.(3.6). The total wavefunction is described as a sum of amplitudes of the rearrangement channels ( $c = 1 \sim 9$ ) of Fig. 3

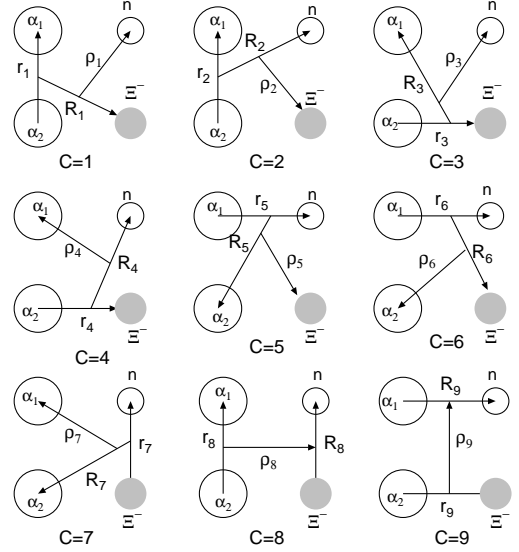


FIG. 3: Jacobian coordinates for all the rearrangement channels ( $c = 1 \sim 9$ ) of the  $\alpha\alpha n\Xi^-$  ( ${}_{\Xi}^{10}\text{Li}$ ) four-body system. Two  $\alpha$  clusters are to be symmetrized. In the case of the  $\alpha nn\Xi^-$  ( ${}_{\Xi}^7\text{H}$ ) four-body system, the two  $\alpha$  clusters are replaced by two neutrons, and the neutron is replaced by an  $\alpha$  cluster.

in the  $LS$  coupling scheme:

$$\begin{aligned} \Psi_{JM, TT_z} ({}_{\Xi}^7\text{H}) &= \sum_{c=1}^9 \sum_{n, N, \nu, l, L, \lambda} \sum_{S, \Sigma, I, K} C_{nlNL\nu\lambda S \Sigma I K}^{(c)} \\ &\times \mathcal{A}_N \left[ \Phi(\alpha) [\chi_{\frac{1}{2}}(\Xi^-) [\chi_{\frac{1}{2}}(n_1) \chi_{\frac{1}{2}}(n_2)]]_S \right]_{\Sigma} \\ &\times \left[ [\phi_{nl}^{(c)}(\mathbf{r}_c) \psi_{NL}^{(c)}(\mathbf{R}_c)]_I \xi_{\nu\lambda}^{(c)}(\boldsymbol{\rho}_c) \right]_K \Big]_{JM} \\ &\times [\eta_{\frac{1}{2}}(\Xi^-) [\eta_{\frac{1}{2}}(n_1) \eta_{\frac{1}{2}}(n_2)]]_{t, T, T_z}, \end{aligned} \quad (5.3)$$

$$\begin{aligned} \Psi_{JM, TT_z} ({}_{\Xi}^{10}\text{Li}) &= \sum_{c=1}^9 \sum_{n, N, \nu, l, L, \lambda} \sum_{S, I, K} C_{nlNL\nu\lambda S I K}^{(c)} \\ &\times \mathcal{S}_{\alpha} \left[ \Phi(\alpha_1) \Phi(\alpha_2) [\chi_{\frac{1}{2}}(n) \chi_{\frac{1}{2}}(\Xi^-)]_S \right] \\ &\times \left[ [\phi_{nl}^{(c)}(\mathbf{r}_c) \psi_{NL}^{(c)}(\mathbf{R}_c)]_I \xi_{\nu\lambda}^{(c)}(\boldsymbol{\rho}_c) \right]_K \Big]_{JM} \\ &\times [\eta_{\frac{1}{2}}(n) \eta_{\frac{1}{2}}(\Xi^-)]_{T, T_z}. \end{aligned} \quad (5.4)$$

Here the operator  $\mathcal{A}_N$  stands for antisymmetrization between the two neutrons.  $\mathcal{S}_{\alpha}$ ,  $\chi_{\frac{1}{2}}(\Xi^-)$  and  $\eta_{\frac{1}{2}}(\Xi^-)$  are defined already in Sec.III.

The Pauli principle involving nucleons belonging to  $\alpha$  and  $x(=n, \alpha)$  is taken into account by the orthogonality condition model (OCM) [20]. The forbidden states in Eq.(3.6) are  $f = 0S$  for  $n$  and  $f = 0S, 1S, 0D$  for  $x = \alpha$ .

We employ the  $V_{\alpha N}$  potential given in Ref.[22] and the AV8 potential [23] for the two-neutron parts. The  $\alpha nn$  ( $\alpha\alpha n$ ) binding energy derived from these potentials



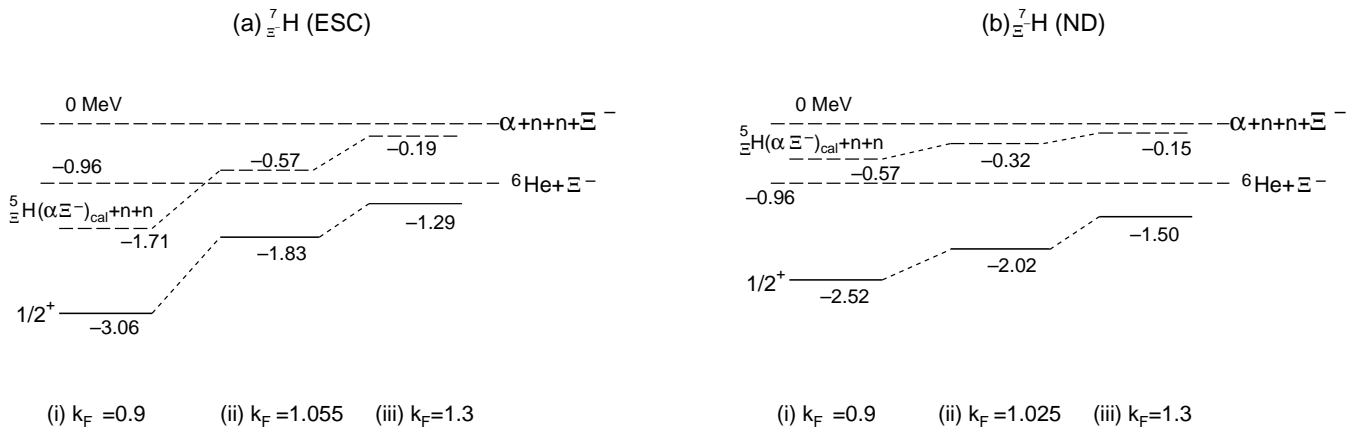


FIG. 4: (a) Calculated energy levels of  ${}^7_{\Xi^-}\text{H}$  for three  $k_F$  values using ESC. (b) Calculated energy levels of  ${}^7_{\Xi^-}\text{H}$  for three  $k_F$  values using ND. The energies are shown when the imaginary part of the  $\alpha\Xi^-$  interaction is switched off. The energies are measured from the  $\alpha+n+n+\Xi^-$  breakup threshold. The dashed lines are threshold.

is less(over) bound by about 0.3 MeV (1 MeV) in comparison with the observed value. Then, in calculations of the  $\alpha nn\Xi^-$  and  $\alpha\alpha n\Xi^-$  four-body model, the central part of  $V_{\alpha n}$  is adjusted so as to reproduce the observed ground state of  ${}^6\text{He}$  and  ${}^9\text{Be}$ . The  $V_{\alpha\alpha}$  and  $V_{\alpha\Xi^-}$  are the same as those in  $\alpha\alpha t\Xi^-$  four-body calculations. As for the  $\Xi^-n$  parts, we employ the simple three-range Gaussian potentials derived from ESC and ND. The details of these potentials were already mentioned in Sec. II. Thus, in our treatments of  $\alpha nn\Xi^-$  and  $\alpha\alpha n\Xi^-$  four-body systems, ground-state energies of all subsystems of  $\alpha nn$  and  $\alpha\alpha n$  are reproduced well.

### B. Results for ${}^7_{\Xi^-}\text{H}$ ( $\alpha nn\Xi^-$ )

Here we describe the results of the four-body calculations for  ${}^7_{\Xi^-}\text{H}(\alpha nn\Xi^-)$  with  $(T, J^\pi) = (3/2, 1/2^+)$ . The basic question is whether this state is bound or not: The  ${}^6\text{He}$  core is composed of an  $\alpha$  and two weakly-bound ('halo') neutrons. Due to the weakness of the  $\Xi^-n$  interaction, the binding between  ${}^6\text{He}$  and  $\Xi^-$  is to a large extent determined by the  $\alpha\Xi^-$  interaction.

The calculated energies in the  $1/2^+$  ground state are demonstrated in Fig. 4 as a function of  $k_F$ , for the two  $\Xi N$  potential models without the imaginary part of the  $\alpha\Xi^-$  interaction. These  $1/2^+$  states are composed of the ground-state  $0^+$  configuration of  ${}^6\text{He}$  coupled with the  $0s$ -state  $\Xi^-$  particle. The Coulomb interactions between  $\alpha$  and  $\Xi^-$  are taken into account. In the figure, the dashed lines show the positions of threshold energies of  $\alpha+n+n+\Xi^-$ ,  ${}^6\text{He}+\Xi^-$  and  ${}^5_{\Xi^-}\text{H}(\alpha\Xi^-)_{\text{cal}}+n+n$ , respectively. One should be aware that the  ${}^5_{\Xi^-}\text{H}(\alpha\Xi^-)_{\text{cal}}+n+n$  threshold energy depends on the  $k_F$  value of the adopted  $\Xi N$  interactions. This situation is unavoidable, because the calculated energies for  ${}^7_{\Xi^-}\text{H}$  have to be used instead of the unknown experimental value. We see that in the case (i)  $k_F = 0.9 \text{ fm}^{-1}$  with ESC the lowest thresh-

old is  ${}^5_{\Xi^-}\text{H}(\alpha\Xi^-)_{\text{cal}}+n+n$ , and in the other cases the  ${}^6\text{He}+\Xi^-$  threshold is lower than the  ${}^5_{\Xi^-}\text{H}(\alpha\Xi^-)_{\text{cal}}+n+n$  threshold. On the other hand, in all  $k_F$  cases with ND the lowest threshold is  ${}^6\text{He}+\Xi^-$ . The order of the  ${}^5_{\Xi^-}\text{H}(\alpha\Xi^-)_{\text{cal}}+n+n$  and  ${}^6\text{He}+\Xi^-$  threshold is determined by the competition between  $\alpha\Xi^-$  correlation and the  $\alpha$ -( $nn$ ) correlation.

More detailed results are given in Table VIII, where the calculated values of the conversion widths  $\Gamma$  and the  $\alpha\Xi^-$  and  $\alpha n$  r.m.s. radii are also listed.

Now, let us compare the results for ESC and ND in the cases in which the imaginary part of the  $\alpha\Xi^-$  interaction is switched off. As found in Table VI (values in parentheses), the obtained  $\alpha\Xi^-$  states for ESC are more bound than those for ND ( $-1.71$  MeV vs.  $-0.57$  MeV for  $k_F = 0.9 \text{ fm}^{-1}$ ). In the  $\alpha nn\Xi^-$  system, however, the energy difference between ESC and ND becomes small in comparison with that in the  $\alpha\Xi^-$  system ( $-3.06$  MeV vs.  $-2.52$  MeV for  $k_F = 0.9 \text{ fm}^{-1}$ ), as shown in Fig. 4 and Table VIII (values in parentheses). This is because the  ${}^{31}S_0$  and  ${}^{33}S_1$   $n\Xi^-$  interactions of ND are more attractive than those of ESC, as shown in Fig. 1. The stronger  $n\Xi^-$  attraction in ND has the effect of a larger reduction of the value of  $\bar{r}_{\alpha-\Xi^-}$  when one goes from the  $\alpha\Xi^-$  system to the  $\alpha nn\Xi^-$  system.

Let us discuss the structure of  ${}^7_{\Xi^-}\text{H}$ . In the case of  $k_F = 0.9 \text{ fm}^{-1}$  for ESC, the lowest threshold is  ${}^5_{\Xi^-}\text{H}(\alpha\Xi^-)_{\text{cal}}+n+n$ . Then, the  $\Xi^-$  particle is bound to the  $\alpha$  particle mostly in the  $0s$  orbit, and the two valence neutrons are coupled to the  $\alpha\Xi^-$  subsystem. In fact, as shown in Table VIII,  $\bar{r}_{\alpha-\Xi^-}$  is shorter than  $\bar{r}_{\alpha-n}$  in this case. In other cases, the two valence neutrons are bound to the  $\alpha$  core, and the  $\Xi^-$  particle is coupled to the  $\alpha nn$  ( ${}^6\text{He}$ ) subsystem, corresponding to where the  $\bar{r}_{\alpha-\Xi^-}$  values are larger than the  $\bar{r}_{\alpha-n}$  values.

In order to see the structure of the  ${}^7_{\Xi^-}\text{H}$  system visually, we draw the density distributions of  $\Xi^-$  (solid curves) and valence neutrons (dashed curves) in Fig. 5(a) and

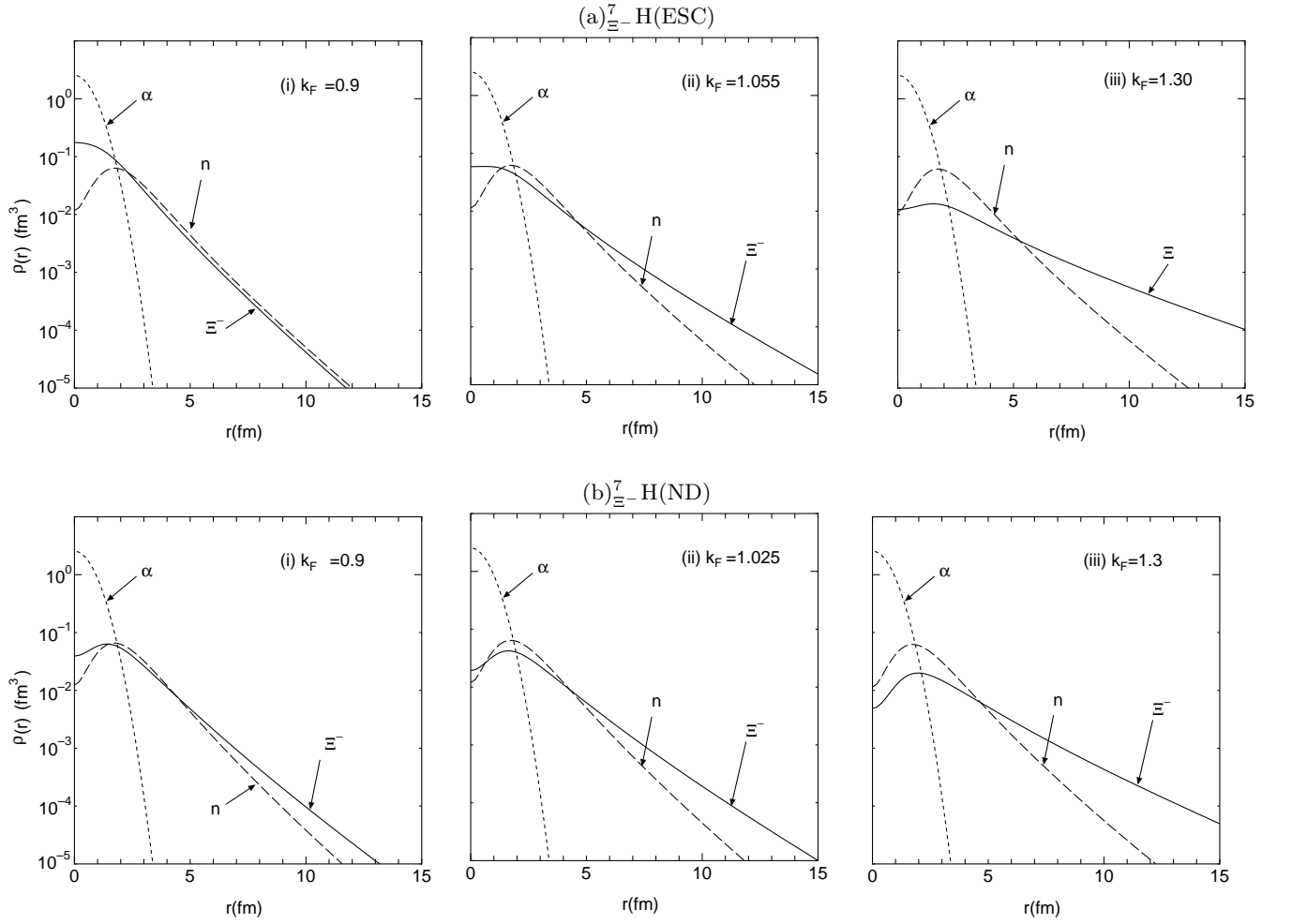


FIG. 5: (a) Calculated density distribution of  $\alpha$ ,  $\Xi^-$  and a valence neutron for three  $k_F$  values using ESC. (b) Calculated density distribution of  $\alpha$ ,  $\Xi^-$  and a valence neutron for three  $k_F$  values using ND. The wavefunctions of  $\alpha\Xi^-$  without the imaginary part of the  $\alpha\Xi^-$  interaction are used.

(b) for ESC and ND, respectively. For comparison, also a single-nucleon density in the  $\alpha$  core is shown by a dotted curve in each case. It turns out, here, that as the binding energies of  ${}^7_{\Xi^-}\text{H}$  become smaller, the  $\Xi^-$  density distribution has a longer tail. As is well known,  ${}^6\text{He}$  is a neutron-halo nucleus. It is interesting here to see the overlapping of the  $\Xi^-$  distribution with the halo-neutron distribution. In the case of  $k_F = 0.9 \text{ fm}^{-1}$  for ESC, since the lowest threshold is  ${}^5_{\Xi^-}\text{H}(\alpha\Xi^-)_{\text{cal}} + n + n$ , the density of the  $\Xi^-$  particle has a shorter-ranged tail than that of the two valence neutrons, but is extended significantly away from the  $\alpha$  core. This situation can be visualized as three layers of matter distribution, the  $\alpha$  core, a  $\Xi^-$  skin, and neutron halo. When the lowest breakup threshold is  ${}^6\text{He} + \Xi^-$ , the  $\Xi^-$  density is longer-ranged than that of the valence neutrons due to the weaker binding of the  $\Xi^-$  particle. Then, the density distribution of  ${}^7_{\Xi^-}\text{H}$  shows the three layers of the  $\alpha$  core, neutron halo, and  $\Xi^-$  halo. Namely, a double-halo structure of neutrons and  $\Xi^-$  ex-

ists, in which the attractive Coulomb interaction plays an essential role. These features can be considered as new forms in baryon many-body systems.

Table VIII lists the binding energies of the  ${}^7_{\Xi^-}\text{H}$  system calculated with and without the Coulomb interaction for each  $k_F$  value. For ESC ( $k_F = 0.9 \text{ fm}^{-1}$ ) and ND ( $k_F = 0.9$  and  $1.025 \text{ fm}^{-1}$ ) the ground states of  ${}^7_{\Xi^-}\text{H}$  are found to be weakly bound states, when the Coulomb interactions are switched off. Therefore, the  ${}^7_{\Xi^-}\text{H}$  systems are seen to have nuclear-bound states, if we take reasonable values  $k_F < 1 \text{ fm}^{-1}$ . This means that an experimental finding of a  ${}^7_{\Xi^-}\text{H}$  bound state indicates the existence of an  $\alpha\Xi^-$  bound state in which the even-state spin-independent part of the  $\Xi N$  interaction is substantially attractive. This statement is almost independent of the interaction model.



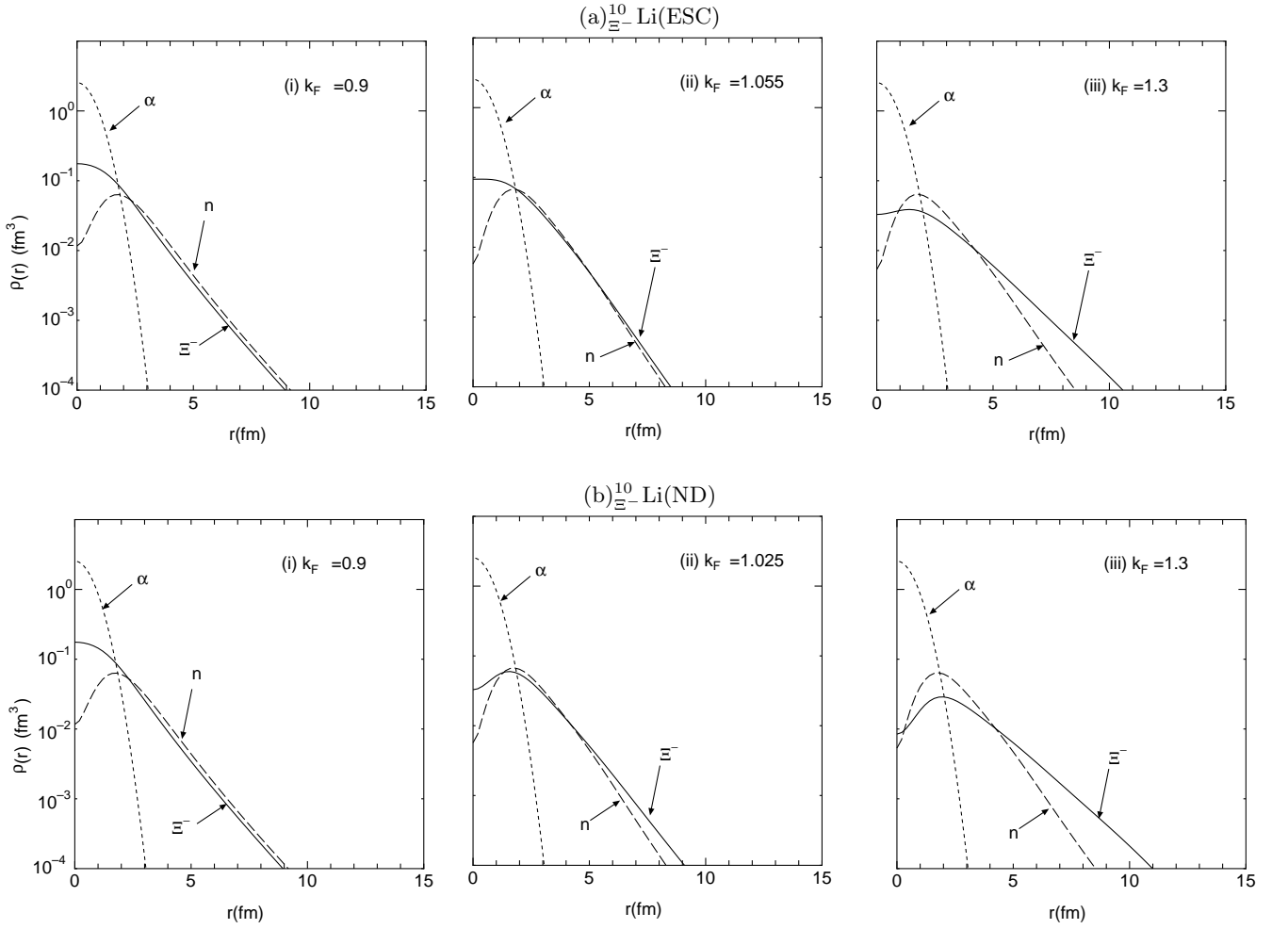


FIG. 7: (a) Calculated density distribution of  $\alpha$ ,  $\Xi^-$ , and a valence neutron for three  $k_F$  values using ESC. (b) Calculated density distribution of  $\alpha$ ,  $\Xi^-$ , and a valence neutron for three  $k_F$  values using ND. The wavefunctions of  $\alpha\Xi^-$  without the imaginary part of the  $\alpha\Xi^-$  interaction are used.

We say that the  $\alpha n\Xi^- (^{10}_{\Xi^-}\text{Li})$  system produced by the  $(K^-, K^+)$  reaction on  $^{10}\text{B}$  is suitable to investigate  $\alpha\Xi^-$  interactions, namely the spin-independent terms of even and odd-state  $\Xi N$  interactions.

## VI. SUMMARY AND OUTLOOK

In anticipation of priority experiments to be done at the J-PARC facility, we have carried out detailed structure calculations for several light p-shell  $\Xi$ -hypernuclei,  $^{12}_{\Xi^-}\text{Be}$ ,  $^5_{\Xi^-}\text{H}$ ,  $^9_{\Xi^-}\text{Li}$ ,  $^7_{\Xi^-}\text{H}$  and  $^{10}_{\Xi^-}\text{Li}$ , in order to investigate whether we can expect the existence of bound states of the  $\Xi^-$  hyperon. The calculational framework is microscopic three- and four-body cluster models using the Gaussian Expansion Method which has been proved to work quite successfully in obtaining reliable numerical solutions.

One of the essential issues in preparing such detailed

calculations is what kind of  $\Xi N$  interactions one should use, because there are no definitive experimental data for any  $\Xi$ -hypernucleus, and also because there are large uncertainties in the spin and isospin dependence in the existing  $\Xi N$  interaction models. The only existing experimental indication, from the  $^{12}\text{C}(K^-, K^+)^{12}_{\Xi^-}\text{Be}$  reaction spectrum, is that the  $^{11}\text{B}-\Xi^-$  interaction is substantially attractive. However this constraint is helpful in excluding most of the  $SU_3$ -invariant  $BB$  interaction models which lead to repulsive  $\Xi$ -nucleus potentials. In this work, we used two  $\Xi N$  potential models, ND and ESC, which give rise to substantially attractive  $\Xi$ -nucleus potentials in accordance with the experimental information. Although the spin- and isospin-components of these two models are very different from each other due to the different meson contributions, we can reliably speak about the spin- and isospin-averaged properties such as  $\bar{G}^{(\pm)} = (G_{00}^{(\pm)} + 3G_{01}^{(\pm)} + 3G_{10}^{(\pm)} + 9G_{11}^{(\pm)})/16$ . This is why we have focused our attention on the  $\alpha$ -cluster based

TABLE VIII: The calculated binding energies of  $1/2^+$ ,  $E$  and r.m.s radii,  $\bar{r}_{\alpha-\Xi^-}$  and  $\bar{r}_{\alpha-n}$ , in the  ${}_{\Xi^-}^7\text{H}(\alpha nn\Xi^-)$  system for several values of  $k_F$ . The values in parentheses are energies when the imaginary part of the  $\alpha\Xi^-$  interactions are switched off. The energies are measured from the  $\alpha + \alpha + n + \Xi^-$  threshold.

(a) ${}_{\Xi^-}^7\text{H}(\text{ESC})$				
with	$k_F(\text{fm}^{-1})$	0.9	1.055	1.3
Coulomb	$E$ (MeV)	-2.76	-1.63	-1.22
		(-3.06)	(-1.83)	(-1.29)
	$\Gamma(\text{MeV})$	2.64	1.15	0.31
	$\bar{r}_{\alpha-\Xi^-}$ (fm)	3.68	5.58	9.92
	$\bar{r}_{\alpha-n}$ (fm)	4.04	4.11	4.19
without	$E$ (MeV)	-1.68	unbound	unbound
Coulomb		(-1.96)	(-1.09)	(unbound)
	$\Gamma(\text{MeV})$	2.09	-	-
(b) ${}_{\Xi^-}^7\text{H}(\text{ND})$				
with	$k_F(\text{fm}^{-1})$	0.9	1.025	1.3
Coulomb	$E$ (MeV)	-2.51	-2.01	-1.50
		(-2.52)	(-2.02)	(-1.50)
	$\Gamma(\text{MeV})$	0.27	0.15	0.032
	$\bar{r}_{\alpha-\Xi^-}$ (fm)	4.48	5.35	7.55
	$\bar{r}_{\alpha-n}$ (fm)	3.92	3.99	4.11
without	$E$ (MeV)	-1.62	-1.26	unbound
Coulomb		(-1.63)	(-1.26)	(unbound)
	$\Gamma(\text{MeV})$	0.22	0.10	-

systems and started with an investigation of the nuclear spin- and isospin-saturated systems such as  $\alpha\Xi^-$  ( ${}_{\Xi^-}^5\text{H}$ ) and  $\alpha\alpha\Xi^-$  ( ${}_{\Xi^-}^9\text{Li}$ ), so as to get a firm basis of our analyses.

However, the pure  $\alpha$ -cluster systems such as  $\alpha\Xi^-$  and  $\alpha\alpha\Xi^-$  cannot be produced directly, because there are no available nuclear targets for the  $(K^-, K^+)$  reaction. Thus, in order to explore realistic experimental possibilities, we have extended the calculation to the four-body  $\Xi^-$ -systems having one or two additional neutrons. This explains why we took the  ${}_{\Xi^-}^7\text{H}(\alpha nn\Xi^-)$  and  ${}_{\Xi^-}^{10}\text{Li}(\alpha\alpha n\Xi^-)$  hypernuclei as the typical  $\Xi^-$ -systems in this paper.

The major conclusions are summarized as follows:

(1) In order to be consistent with the existing experimental indication that the  $\Xi$ -nucleus interaction is attractive, the fine tuning of the ND and ESC potential models has been made for applications to  $\Xi$ -hypernuclei by adjusting the hard-core radius  $r_c$  in ND and the  $\alpha_V$  parameter for the medium-induced effect in ESC, respectively. Then the  $\Xi N$  G-matrices were derived and represented in terms of three-range Gaussians with the  $k_F$  parameter expressing its density-dependence within the

TABLE IX: The calculated binding energies,  $E$  of the  $1_1^-$  and  $2_1^-$  states in the  ${}_{\Xi^-}^{10}\text{Li}(\alpha\alpha n\Xi^-)$  system for several values of  $k_F$ . The values in parentheses are energies when the imaginary part of the  $\alpha\Xi^-$  interactions are switched off. The energies are measured from the  $\alpha + \alpha + n + \Xi^-$  threshold. The calculated r.m.s. radii,  $\bar{r}_{\alpha-\Xi^-}$ ,  $\bar{r}_{\alpha-n}$  and  $\bar{r}_{\alpha-\alpha}$  of  $2^-$  state using ESC and ND.

(a) ${}_{\Xi^-}^{10}\text{Li}(\text{ESC})$				
with Coulomb	$k_F(\text{fm}^{-1})$	0.9	1.055	1.30
$2^-$	$E$ (MeV)	-7.99	-4.83	-2.87
		(-8.35)	(-5.16)	(-3.13)
	$\Gamma(\text{MeV})$	5.87	3.63	1.71
	$\bar{r}_{\alpha-\Xi^-}$ (fm)	3.05	3.72	5.03
	$\bar{r}_{\alpha-n}$ (fm)	3.55	3.70	3.83
	$\bar{r}_{\alpha-\alpha}$ (fm)	3.25	3.41	3.54
$1^-$	$E$ (MeV)	-7.48	-4.42	-2.64
		(-7.84)	(-4.77)	(-2.89)
	$\Gamma(\text{MeV})$	5.72	3.44	1.50
without Coulomb	$E$ (MeV)	-5.54	-2.76	-1.41
$2^-$		(-5.93)	(-3.14)	(-1.63)
	$\Gamma(\text{MeV})$	5.39	3.00	1.10
(b) ${}_{\Xi^-}^{10}\text{Li}(\text{ND})$				
with Coulomb	$k_F(\text{fm}^{-1})$	0.9	1.025	1.3
$2^-$	$E$ (MeV)	-5.83	-4.42	-2.92
		(-5.85)	(-4.43)	(-2.92)
	$\Gamma(\text{MeV})$	0.75	0.42	0.10
	$\bar{r}_{\alpha-\Xi^-}$ (fm)	3.55	4.10	5.40
	$\bar{r}_{\alpha-n}$ (fm)	3.64	3.72	3.83
	$\bar{r}_{\alpha-\alpha}$ (fm)	3.35	3.44	3.54
$1^-$	$E$ (MeV)	-5.98	-4.53	-2.97
		(-5.99)	(-4.53)	(-2.97)
	$\Gamma(\text{MeV})$	0.77	0.43	0.10
without Coulomb	$E$ (MeV)	-3.75	-2.60	-1.54
$2^-$		(-3.76)	(-2.61)	(-1.54)
	$\Gamma(\text{MeV})$	0.62	0.32	0.005

nucleus. The  $\Lambda\Lambda - \Xi N - \Sigma\Sigma$  coupling term in the bare interaction is renormalized into the imaginary part in the G-matrix interactions

(2) First we performed the  $\alpha\alpha t\Xi^-$  four-body calculation of  ${}_{\Xi^-}^{12}\text{Be}$  and found that  $k_F = 1.055\text{fm}^{-1}$  for  $G_{\text{ESC}}$  and  $1.025\text{fm}^{-1}$  for  $G_{\text{ND}}$  are most appropriate to produce the  $B_{\Xi^-}^{\text{CAL}}(J = 1^-) = 2.2\text{ MeV}$  (without Coulomb interaction) which is that suggested empirically. These values around  $k_F \sim 1.0\text{ fm}^{-1}$  are reasonable, because they agree roughly with the values estimated from the average density in a  $A \cong 12$  nucleus. Then, we naturally allow smaller  $k_F$  values for smaller mass numbers.

(3) In the basic structure calculations for  $\alpha\Xi^-$  ( ${}_{\Xi^-}^5\text{H}$ )

and  $\alpha\alpha\Xi^-$  ( ${}^9\text{Li}$ ) systems, we have tested three values of  $k_F$  parameters,  $k_F = 0.9, 1.055$  and  $1.3$  for ESC and  $k_F = 0.9, 1.025$  and  $1.3$  for ND, respectively. In the  $\alpha\Xi^-$  system, for which  $k_F \simeq 0.9 \text{ fm}^{-1}$  is considered to be reasonable, we obtained only Coulomb-assisted bound states with small binding energies, since they disappear without the Coulomb interaction. In the  $\alpha\alpha\Xi^-$  system, on the other hand, nuclear bound states are obtained for the acceptable range of  $k_F$  between  $0.9 \text{ fm}^{-1}$  and  $1.05 \text{ fm}^{-1}$ . The calculated binding energies of ESC are larger than those of ND, and also the  $k_F$ -dependence is more sensitive in ESC. If these predictions are confirmed, directly or indirectly, in future experiments, then it will provide a good check for the spin- and isospin-averaged  $\Xi N$  interaction strengths.

(4) For the lightest realistic example,  ${}^7_{\Xi}\text{H}(\alpha nn\Xi^-)$ , the four-body calculation predicts the existence of nuclear bound states in both cases of ESC and ND at reasonable  $k_F$  values of around  $0.9 \text{ fm}^{-1}$ . It is interesting to note that the addition of two neutrons to the  $\alpha\Xi^-$  system gives rise to about 1.3 (2.0) MeV more binding for the ESC (ND) cases, respectively. If the experiment is carried out to observe the  ${}^7_{\Xi}\text{H}$  bound states, it is useful to extract information about the even-state spin- and isospin-averaged part of the  $\Xi N$  interaction acting between the  $\alpha$  and  $\Xi^-$ .

(5) For the second realistic example, the  ${}^{10}_{\Xi}\text{Li}(\alpha\alpha n\Xi^-)$  hypernucleus, we have obtained the nuclear  $\Xi^-$  bound states as a result of careful four-body calculations with  $k_F \sim 1.0 \text{ fm}^{-1}$ . This result is essentially based on the averaged attractive nature of the  $\Xi N$  interactions acting

in the three-body subsystem of  $\alpha\alpha\Xi^-$ . It is remarkable to have similar binding energies of the  $J = 2^-$  state for both the ESC and ND interactions ( $-4.8 \text{ MeV}$  vs.  $-4.4 \text{ MeV}$  with respect to the  $\alpha + \alpha + n + \Xi^-$  threshold). The order of the doublet states ( $J = 1^-, 2^-$ ) is calculated to be opposite for ESC and ND as a result of the difference in the  ${}^{31}S_1$  and  ${}^{33}S_0$  components of ESC and ND acting between the  $\Xi^-$  and a neutron.

In conclusion, it will be quite interesting to observe the newly predicted bound states in future ( $K^-, K^+$ ) experiments using the  ${}^7\text{Li}$  and  ${}^{10}\text{B}$  targets in addition to the standard  ${}^{12}\text{C}$  target. Experimental confirmation of these states will surely provide us with definite information on the spin- and isospin-averaged  $\Xi N$  interactions; note the information on its even-state part from  $\alpha\Xi^-$  and  $\alpha\alpha\Xi^-$  and its odd-state part from  $\alpha\alpha\Xi^-$ . Such a plan is a challenging project in the study of  $\Xi$ -hypernuclei that have yet to be explored. In order to convert the present predictions into concrete experimental proposals at J-PARC, the reaction cross sections should be estimated for the  ${}^7\text{Li}(K^-, K^+)_{\Xi^-}{}^7\text{H}$ ,  ${}^{10}\text{Li}(K^-, K^+)_{\Xi^-}{}^{10}\text{Li}$  and  ${}^{12}\text{C}(K^-, K^+)_{\Xi^-}{}^{12}\text{Be}$  reactions.

#### Acknowledgments

The authors thank B. F. Gibson for helpful discussions. This work was supported by a Grant-in-Aid for Scientific Research from Monbukagakusho of Japan. The numerical calculations were performed on the HITACHI SR11000 at KEK.

- 
- [1] P. Khaustov *et al.*, Phys. Rev. **C61**, (2000) 054603.  
[2] S. Aoki *et al.*, Prog. Theor. Phys. **89** (1993), 493.; S. Aoki *et al.*, Phys. Lett. **B355** (1995), 45.; Y. Yamamoto, Genshikaku Kenkyu 39 (1996), 23.  
[3] M. M. Nagels, T. A. Rijken, and J. J. deSwart, Phys. Rev. **D15** (1977) 2547.  
[4] Th. A. Rijken and Y. Yamamoto, Phys. Rev. **C73**, 044008 (2006); [arXiv:nucl-th/0603042]  
[5] Th. A. Rijken and Y. Yamamoto, [arXiv:nucl-th/0608074]  
[6] E. Hiyama, M. Kamimura, T. Motoba, T. Yamada and Y. Yamamoto, Phys. Rev. **C53**, 2075 (1996).  
[7] E. Hiyama, M. Kamimura, T. Motoba, T. Yamada and Y. Yamamoto, Prog. Theor. Phys. **97**, 881 (1997).  
[8] E. Hiyama, M. Kamimura, K. Miyazaki and T. Motoba, Phys. Rev. **C59**, 2351 (1999).  
[9] E. Hiyama, M. Kamimura, T. Motoba and T. Yamada, and Y. Yamamoto, Phys. Rev. Lett. **85**, 270 (2000).  
[10] E. Hiyama, M. Kamimura, T. Motoba and T. Yamada, and Y. Yamamoto, Phys. Rev. **C65**, 011301(R) (2002).  
[11] E. Hiyama, M. Kamimura, T. Motoba and T. Yamada, and Y. Yamamoto, Phys. Rev. **C66**, 024007 (2002).  
[12] E. Hiyama, M. Kamimura, T. Motoba and T. Yamada, and Y. Yamamoto, Phys. Rev. **C74**, 054312 (2006).  
[13] Y. Yamamoto and Th. A. Rijken, Nucl. Phys. A **804**, 139 (2008).  
[14] M. Yamaguchi, K. Tominaga, Y. Yamamoto and T. Ueda, Prog. Theor. Phys. **105** (2001) 627  
[15] M. Kamimura, Phys. Rev. **A38**, 621 (1988).  
[16] H. Kameyama, M. Kamimura and Y. Fukushima, Phys. Rev. **C40**, 974 (1989).  
[17] E. Hiyama, Y. Kino and M. Kamimura, Prog. Part. Nucl. Phys. **51**, 223 (2003).  
[18] A. Hasegawa and S. Nagata, Prog. Theor. Phys. **45**, 1786 (1971).  
[19] H. Furutani, H. Kanada, T. Kaneko, S. Nagata, H. Nishioka, S. Okabe, S. Saito, T. Sakuda, and M. Seya, Prog. Theor. Phys. Suppl. **68**, 193 (1980).  
[20] S. Saito, Prog. Theor. Phys. **41**, 705 (1969).  
[21] V. I. Kukulin, V. N. Pomerantsev, Kh. D. Razikov, V. T. Voronchev, and G. G. Ryzhinkh, Nucl. Phys. **A586**, 151 (1995).  
[22] H. Kanada, T. Kaneko, S. Nagata, and M. Nomoto, Prog. Theor. Phys. **61**, 1327 (1979).  
[23] B. S. Pudliner, V. R. Pandharipande, J. Carlson, S. C. Pieper, and R. B. Wiringa, Phys. Rev. C **56**, 1720, (1997).